Research article

Rapports De Pharmacie Vol.1 (3), 2015, 136-149
ISSN: 2455-0507

THE EFFECT OF CHOLESTEROL AND NON IONIC SURFACTANTS ON SILYMARIN NIOSOMES: PARTICLE SIZE, CUMULATIVE DRUG RELEASE AND ENTRAPMENT EFFICIENCY

Logeswary.K[1], Jaya Raja Kumar[2]

[1]*Research student of Pharmacy, AIMST University, Semeling, Bedong, Malaysia*
[2]*Faculty of Pharmacy, AIMST University, Semeling, Bedong, Malaysia*

ABSTRACT

The aim of the present research work was to develop silymarin (SM) loaded nanostructured lipid carriers by ether injection method. In this work, we report the effect on the formulation of silymarin niosomes. Through preliminary experiments the Cholesterol (A), Tween 80 (B) and Span 80 (C) were identified as the most significant variables influence the particle size, % CDR, % entrapment efficiency and viscosity. Silymarin niosomes were analyzed by three-factor, three-level Box-Behnken factorial design. In this study two dependent variables % of CDR and particle size were measured as responses. At low levels of A, R1 reduced from 806 to 804 nm. Similarly at high levels of A, R1 reduced from 910 to 904 nm. The "PredR^2" of 0.9995 is in reasonable agreement with the adj R-Squared of 0.99998. Adeq precision measures the signal to noise ratio. A ratio greater than 4 is desirable. "Adeq precision" (R1, R2, R3 and R4) was 260.621, 116.230, 91.903 and 379.858 indicates an adequate signal respectively.

Keywords: Silymarin, Niosomes, HPLC, Box-Cox Plot, Quadratic model, HPLC

INTRODUCTION

Silymarin is a mixture of flavonolignans including silybin (the major constituent), isosilybin, silychristin, silydianin, and taxifoline, generally found in the dried fruit of the milk thistle plant, Silybum marianum. Silymarin is an antioxidant and hepato protectant; pretreatment through the material has been stated to increasesynthesis of DNA, RNA, protein, and cholesterol suggesting there generation of hepatectomized liver [1–3]. Silymarin protects liver cells by improving membrane permeability via inhibiting lipidperoxidation [4] and preventing glutathione depletion [5]. Silymarin may mitigate burn-induced oxidative injury in skin [6] and rat brain [7],prevent sepsis induced by acute brain and lung injury [8], and protect against UV radiation caused oxidative damageand carcinogenesis in animal models and skin cells [9,10].

Innumerable potent lipophilic drugs exhibit low oral bioavailability due to their poor aqueous solubility and cannot be delivered via the oral route of administration in their innovative form due to instability, low membrane permeability, poor solubility and efflux transport mechanisms, etc. [11]. In recent years, lipid-based formulations (incorporation of the active lipophilic component into inert lipid vehicles) are used to improve the oral bioavailability of lipophobic drug compounds, which include micro or nanoemulsions, oils, self-emulsifying formulations, surfactant dispersions, liposomes, solid lipid nanoparticles and lipid nanocarriers etc.

Address for correspondence:
Logeswary.K
Research student of Pharmacy ,
AIMST University, Semeling, Bedong,
Malaysia.

Niosomes are self-assembly of non-ionic surfactants which are look like liposomes in their architecture and can be used as an effective alternative to liposomal drug carriers [12]. Niosomes are biodegradable, biocompatible, and nontoxic and are efficient of encapsulating huge quantities of material in a relatively small volume of vesicles [13]. In addition, niosomes are multipurpose carrier systems that can be administered through numerous routes with intramuscular route [14], intravenous injection [15], peroral delivery [16], ocular delivery [17], pulmonary delivery [18] and transdermal delivery [19]. Particular efforts have been designed at using niosomes as effective dermal and transdermal drug delivery systems [20, 21].

INVITRO EVALUATION OF NIOSOMES

Particle size analysis:

Particle size of nanoparticles was determined using malvern particle size analyzer (Zetasizer 4000S, Japan).

Viscosity Studies:

The rheological studies were performed by using brookfieldviscometer (DVII+ Model pro II type- USA). The viscosity of niosomes was determined at 0.3 rpm and means of two readings were used to estimate the viscosity [22].

Drug entrapment efficiency:

The entrapment efficiency was determined using the ultra-centrifugation method with a slight alteration [23]. Briefly, one milliliter of niosomes was centrifuged (Avanti®J-26 XPIcentrifuge) at 82,000×gfor 3 hours at 4◦C using a refrigerated ultracentrifuge so as to separate the niosomes from the non-entrapped drug. Concentration of the free drug was determined using the aforementioned HPLC method (Figure 35). RP HPLC chromatographic separation was performed on a Shimadzu liquid chromatographic system equipped with a LC-20AD solvent delivery system (pump), SPD-20A photo diode array detector, and SIL-20ACHT injector with 50µL loop volume. The LC solution version 1.25 was used for data collecting and processing (Shimadzu, Japan). The HPLC was carried out at a flow rate of 1.0 ml/min using a mobile that is phase constituted of acetonitrile, 5 mm ammonium acetate: methanol (pH 4.5) (25:75, v/v), and detection was made at 278 nm. The mobile phase was prepared daily, filtered through a 0.45µm membrane filter (Millipore) and sonicated before use. A Thermo C18 column (25cm × 4.6mm i.d., 5µ) was used for the separation. The % of drug entrapment in niosomes was calculated according to the following equation[24]:

$$\text{Drug Entrapment \%} = \left[\frac{\text{Total Drug} - \text{Drug in supernatant}}{\text{Total Drug}}\right] \times 100$$

In vitro release studies:

The release of silymarinfrom niosomes was examinedunder sink conditions [25]. Accurate amount of niosomeswereplaced in dialysis bags and suspended in 50 mL of phosphate buffersaline (PBS, pH 7.4) at 37˚C, under magnetic stirring. At pre-determined time intervals, 5 mL of solution was withdrawn andthe volume of receptor compartment was maintained with anequal volume of fresh PBS. The amountof drug present in the samples was determined by HPLC method.

Experimental design:

In this work, we report the successful effect on the formulation of silymarinnoisomes. Through preliminary experiments the Cholesterol (A), Tween 80 (B) and Span 80 (C) were identified as the most significant variables influence the particle size, % CDR, % entrapment efficiency and viscosity. Among various design approaches, the Box-Behnken (BBD) has good design properties, little collinearity, rotatable or nearly rotatable; some have orthogonal blocks, insensitive to outliers and missing data. Does not predict well at the corners of the design space. Use when region of interest and region of operability nearly the same. This Box-Behnken design is appropriate for exploring quadratic response surfaces and constructing second order polynomial models. The BBD consists of simulated center points and the set of points lying at the midpoint of each edge of the multi-dimensional cube.

Seventeen runs were essential for the response surface methodology based on the BBD. Based on the experimental design, the factor combinations produced different responses as presented in Table 2. These results clearly indicate that all the dependent variables are strongly dependent on the selected independent variables as they show a wide variation among the 17 runs. Data were analyzed using Stat-Ease Design-Expert software (DX9) to obtain analysis of variance (ANOVA), regression coefficients and regression equation. Mathematical relationship generated using multiple linear regression analysis for the studied variables are expressed as shown in Table 3.

RESULTS AND DISCUSSION

These equations represent the quantitative effect of Cholesterol (A), Tween 80 (B) and Span 80 (C) and their interaction on Particle size (R1), % CDR (R2), % EE (R3) and Viscosity (R4). The values of the coefficient A, B and C are related to the effect of these variables on the responses R1, R2, R3 and R4.Coefficients with more than one factor term and those with higher order terms represent interaction terms and quadratic relationship respectively. A positive sign represents a synergistic effect, although a negative sign specifies an antagonistic effect. A backward elimination procedure was espoused to fit the data to the quadratic model. Both the polynomial equations were found to be statistically significant ($P < 0.01$), as determined using ANOVA (Table 3, 5, 6&7), as per the provision of Design Expert software (DX9).

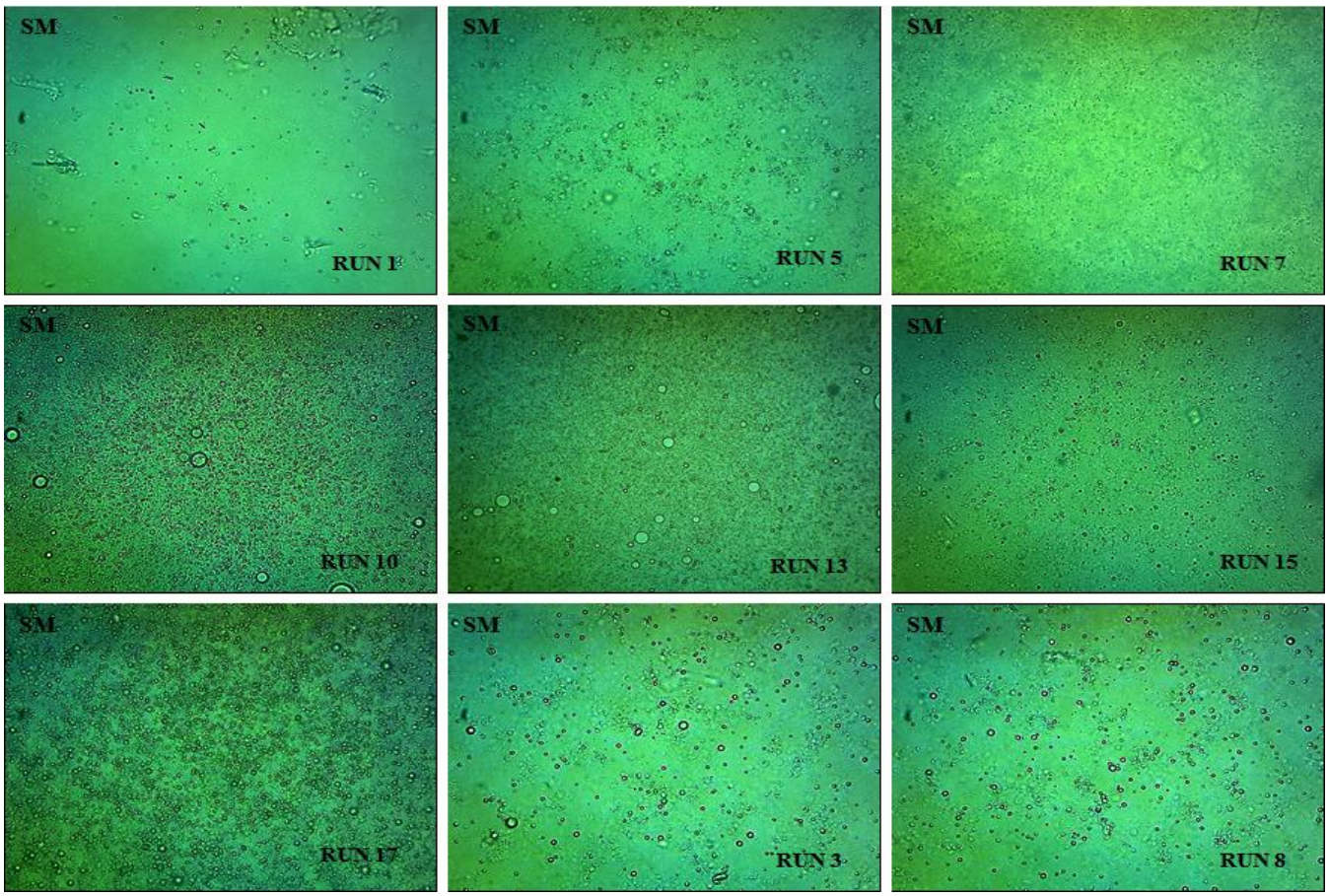

Figure-1: Optical microscopy view of various batches

Preparation of silymarin niosomes:

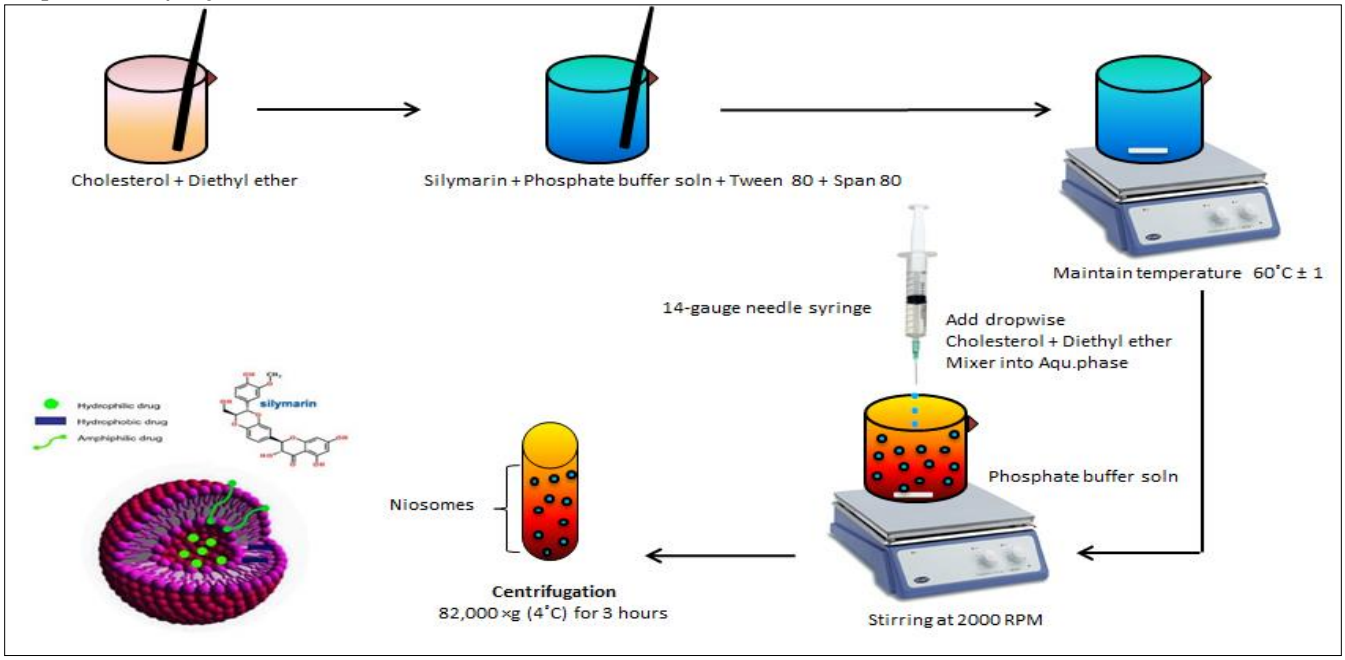

Figure-2: Preparation of silymarin niosomes

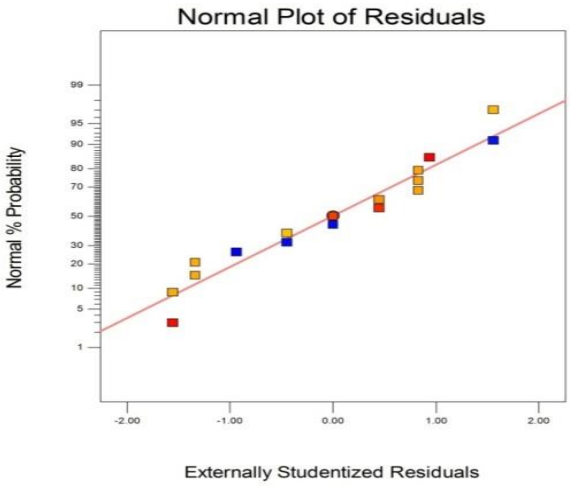

Figure-3: Normal % probability plot of the externally studentizedresiduals (R1)

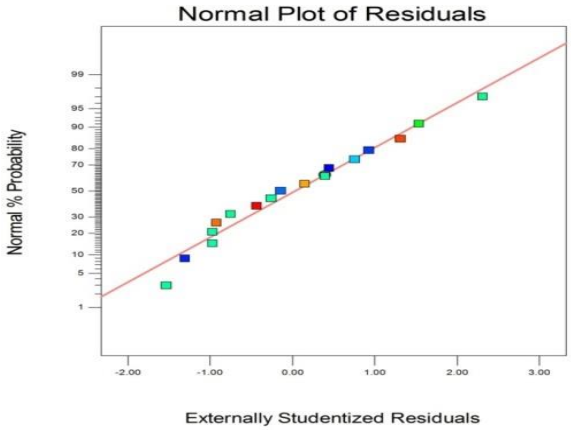

Figure-4: Normal % probability plot of the externally studentized residuals (R2)

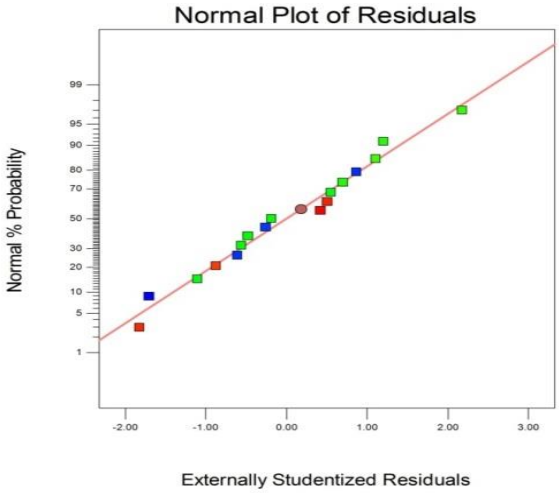

Figure-5: Normal % probability plot of the externally studentized residuals (R3)

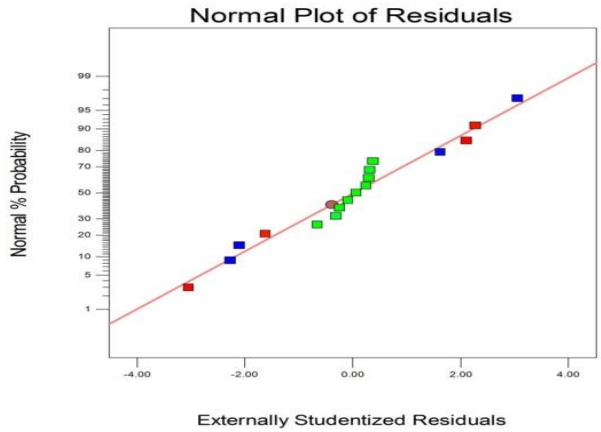

Figure-6: Normal % probability plot of the externally studentized residuals (R4)

The normality of the data could be proved through the normal % probability plot of the externally studentized residuals. If the points on the plot lie on a straight line, the residuals are normally distributed as confirmed in Fig. 3, 4, 5 and 6.

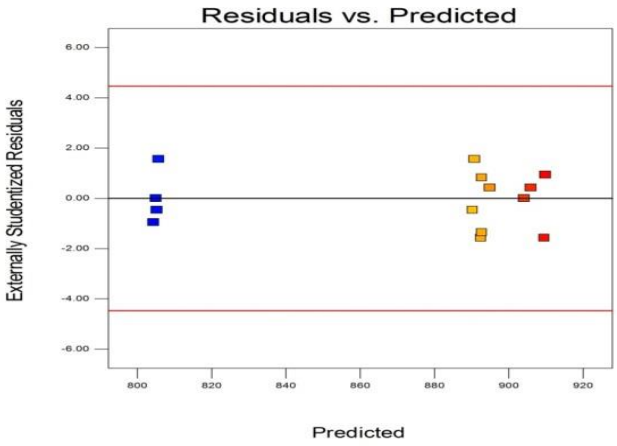

Figure-7: Residuals vs. Predicted (R1)

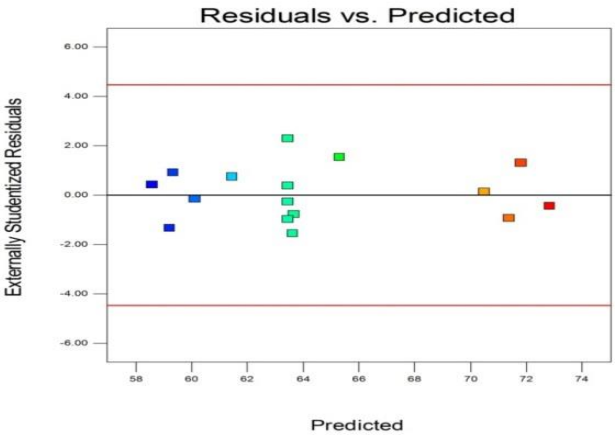

Figure-8: Residuals vs. Predicted (R2)

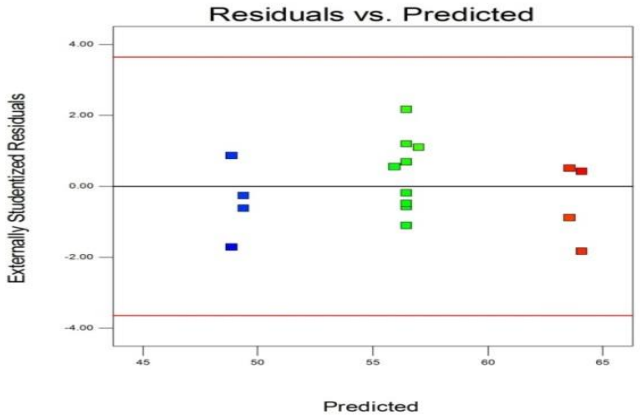

Figure-9: Residuals vs. Predicted (R3)

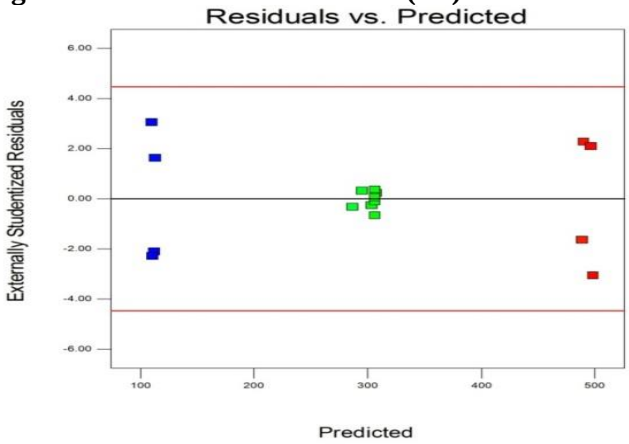

Figure-10: Residuals vs. Predicted (R4)

The assumption of constant variance was tested by plotting externally studentized residual versus predicted values as illustrated in above figures. The studentized residuals are located by dividing the residuals by their standard deviations. According to evident from this figure 7, 8 9 and 10, the points are scattered randomly between the outlier detection limits - 4.5 to + 4.5 and -3.5 to +3.5.

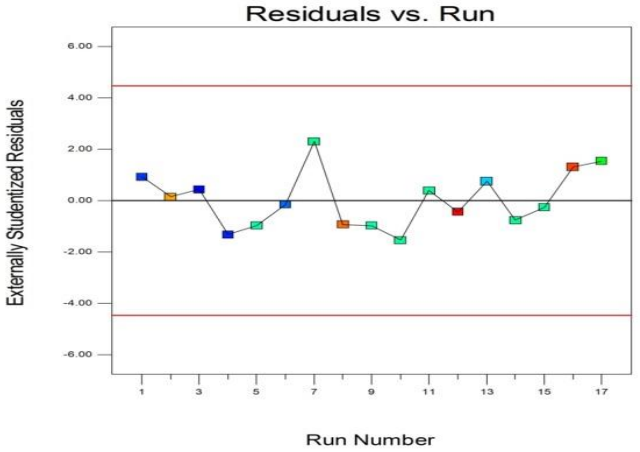

Figure -11: Residuals vs. Run (R1)

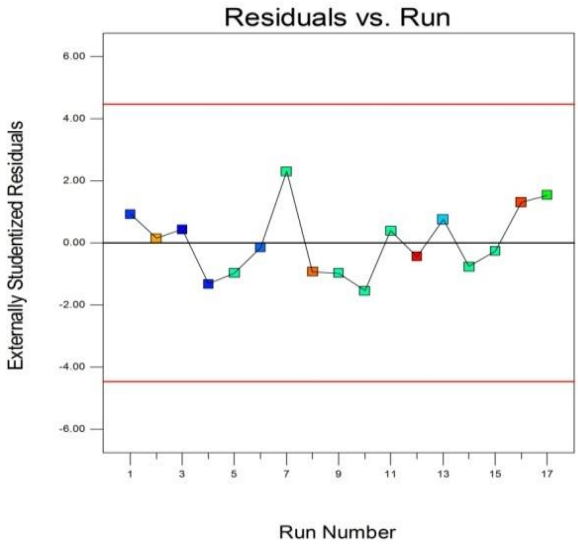

Figure -12: Residuals vs. Run (R2)

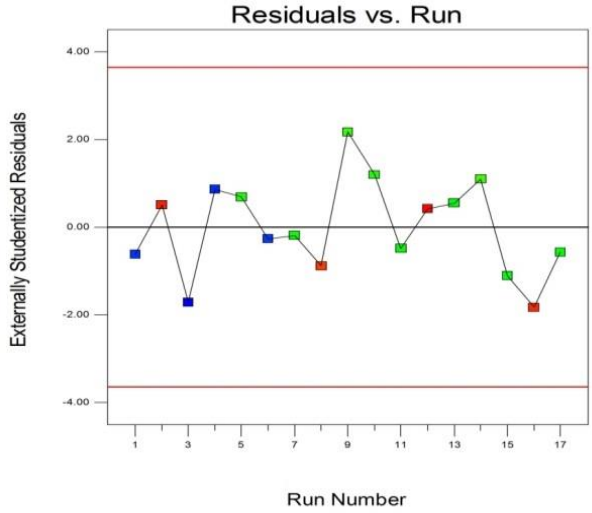

Figure - 13: Residuals vs. Run (R3)

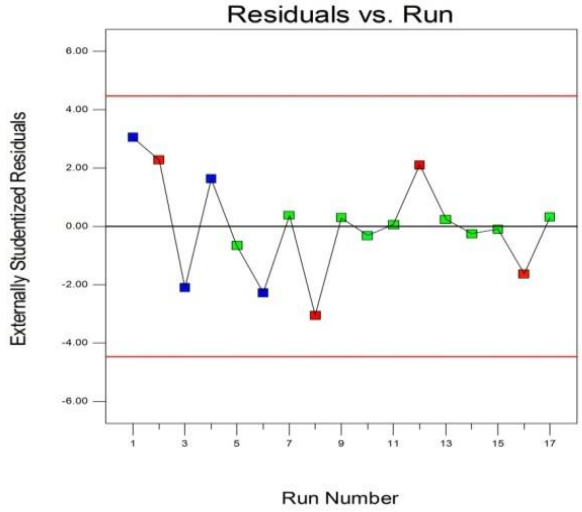

Figure - 14: Residuals vs. Run (R4)

The Residuals Vs. Predicted and Residuals Vs. Run were scattered randomly. From the results it can therefore be seen that the model is suitable for use and can be used to identify the optimalparameters.
R1, R2, R3 and R4 results are quite satisfactory. Also, a high correlation between observed and predicted data indicates their low discrepancies.

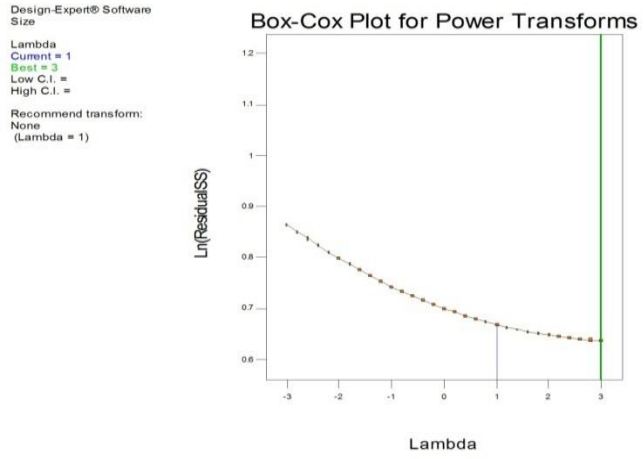

Figure -15: Box-Cox Plot (R1)

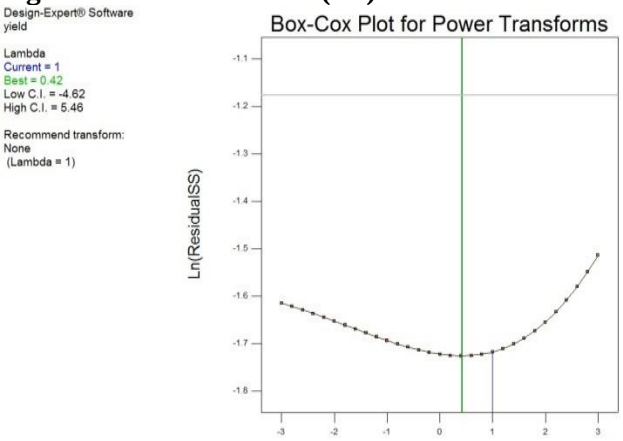

Figure -16: Box-Cox Plot (R2)

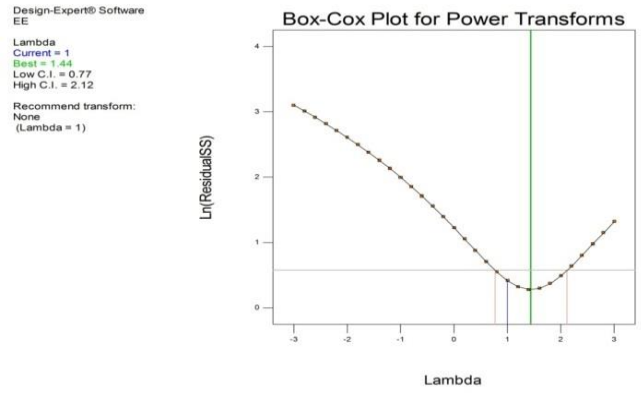

Figure -17: Box-Cox Plot (R3)

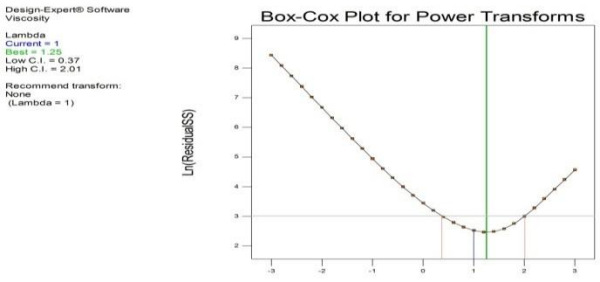

Figure -18: Box-Cox Plot (R4)

The transformation parameter, λ, is chosen such that it maximizes the log-likelihoodfunction. The maximum likelihood estimate of λ agrees to the value for which thesquared sum of errors from the fitted model is a minimum. This value of λ is determined byfitting a numerous values of λ and choosing the value corresponding to the minimumsquared sum of errors. t can also be chosen graphically from the Box-Cox normality plot.Value of λ = 1.00 indicates that no transformation needed and produces results identical to original data shown in Figure 15 to 18.
Particle size analysis of silymarin noisomes was found to be in the range of 804 – 910 nm as shown in Table 2.The factorial equation for particle size exhibited a good correlation coefficient (1.000) and the Model F value of 10570.43 which implies the model is significant. Values of "Prob> F" less than 0.0500 indicate model terms are significant. In this case A, B, C, AB, AC, A^2, B^2 are significant model terms as shown in Table 3. Results of the equation indicate that the effect of Cholesterol (A) and Tween 80 (B) are more significant than C. The influence of the main and interactive effects of independent variables on the particle size was further elucidated using the perturbation and 3D response surface plots. The individual main effects of A, B and C on particle size are as shown in Figure 19. It is found that all the variables are having interactive effects for the response R1. The 3D response surfaces and the 2D contour plots of the response R1 are shown in Figure 20&21 to depict the interactive effects of independent variables on response R1, one variable was kept constant whereas the other two variables diverse in a certain range. The shapes of response surfaces and contour plots reveal the nature and extent of the interaction between different factors. The interaction between A and B on particle size at a fixed level of C is shown in Figure 18. At low levels of A, R1 reduced from 806 to 804 nm. Similarly at high levels of A, R1 reduced from 910 to 904 nm.

The 3-D cube plots of Box-Behnken design are as shown in Figure 21.

Table-1: List of Independent variable and Dependent variables in Box-Behnken design

Independent variable	**Levels**				
Variable	Name	Units	Low	Middle	High
A	Cholesterol	mg	100	175	250
B	Tween 80	mg	100	300	500
C	Span 80	mg	100	300	500
Dependent variable	**Goal**				
R1	Size	nm		Minimize	
R2	CDR	%		Moderate	
R3	EE	%		100	
R4	Viscosity	cps		Moderate	

Table-2: Factorial design of silymarin noisomes formulations

Run	Factor 1 A:Cholestrol mg	Factor 2 B:Tween 80 mg	Factor 3 C:Span 80 mg	Response 1 Size nm	Response 2 CDR at 12 ho.. %	Response 3 EE %	Response 4 Viscosity cps
1	100	300	100	805	59.4	49.2	111.3
2	250	100	300	910	70.5	63.7	491.1
3	100	100	300	805	58.6	48.4	110.6
4	100	300	500	806	59.1	49.1	113.5
5	175	300	300	893	63.3	56.7	305.4
6	100	500	300	804	60.1	49.3	109.1
7	175	300	300	893	63.7	56.4	306.7
8	250	300	500	906	71.3	63.3	496.9
9	175	300	300	893	63.3	57.1	306.6
10	175	100	100	895	63.5	56.8	286.2
11	175	300	300	892	63.5	56.3	306.3
12	250	500	300	904	72.8	64.2	497.8
13	175	100	500	892	61.5	56.1	307.2
14	175	500	100	891	63.6	57.3	303.4
15	175	300	300	892	63.4	56.1	306.1
16	250	300	100	909	71.9	63.6	487.7
17	175	500	500	890	65.4	56.3	295.4

Table-3: ANOVA results of the quadratic model for the response particle size (R1)

Source variations	Sum of Squares	DF	Mean Square	F Value	p-value Prob> F	R^2
Model	26501.58	9	2944.62	10570.43	< 0.0001	0.9999
A-Cholesterol	20910.12	1	20910.12	75061.99	< 0.0001	
B-Tween 80	21.13	1	21.13	75.83	< 0.0001	
C-Span 80	4.50	1	4.50	16.15	0.0051	
AB	6.25	1	6.25	22.44	0.0021	
AC	4.00	1	4.00	14.36	0.0068	
BC	1.00	1	1.00	3.59	0.1000	
A^2	5510.02	1	5510.02	19779.57	< 0.0001	
B^2	1.92	1	1.92	6.89	0.0342	
C^2	0.024	1	0.024	0.085	0.7791	
Residual	1.95	7	0.28			

Lack of Fit	0.75	3	0.25	0.83	0.5413

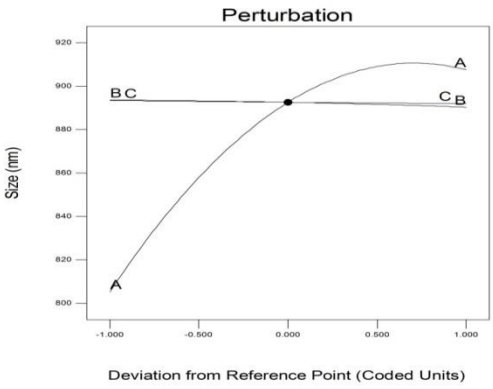

Figure-19: Perturbation plot showing the main effect of cholesterol (A), tween 80 (B) and span 80 (C) on particle size (Y1)

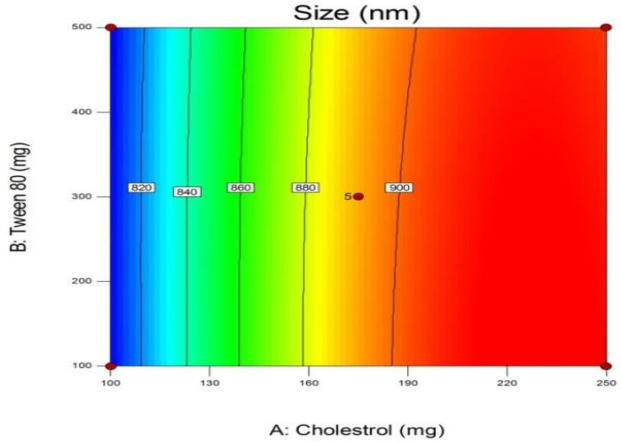

Figure- 20: Response surface plot presenting the interactionbetween the cholesterol and tween 80 affecting the particle size at constant span 80 concentration.

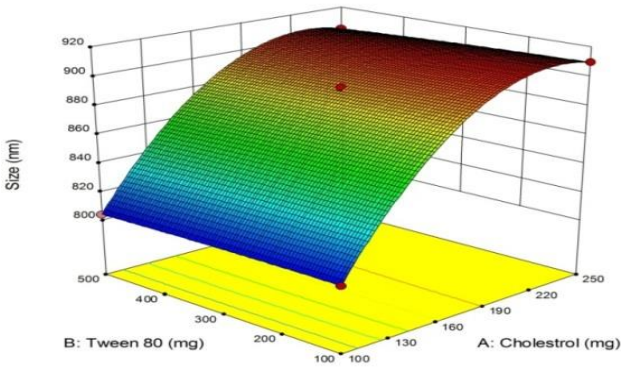

Figure -21: Response surface plot presenting the interactionbetween the cholesterol and tween 80 affecting the particle sizeat constant span 80 concentration.

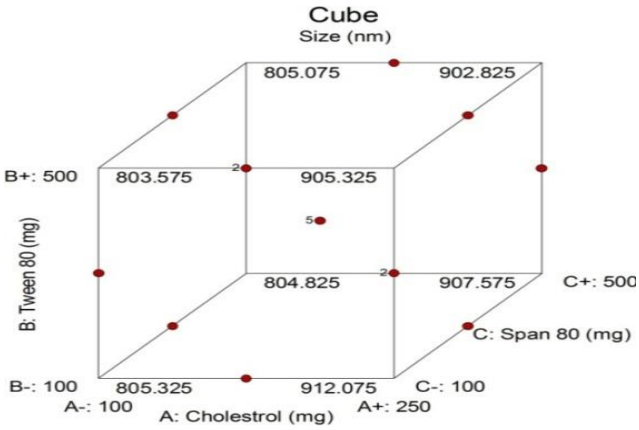

Figure -22: 3-D cube plot of Box-Behnken design

The coefficient of determination, R-squared, is a measure of the fraction of the total squared error that is explained by the model. By definition the value of R^2 varies between zero and one and the closer it is to one, the better. However, a large value of R^2 does not necessarily imply that the regression model is good one. Adding a variable to the model will always increase R^2, regardless of whether the additional variable is statistically significant or not. Thus it is possible for models that have large values of R^2 to CDR poor predictions of new observations or estimates of the mean response. To avoid this confusion, an extra statistic called the Adjusted R-squared statistic is needed; its value decreases if unnecessary terms are added. These two statistics can, when used together, imply the existence of extraneous terms in the computed model which is indicated by a large difference, usually of more than 0.20, between the values of R^2 and Adj-R^2. The amount by which the output predicted by the model differs from the actual output is called the residual. Predicted Residual Error Sum of Squares (PRESS) is a measure of how the model fits each point in the design. It is used to calculate predicted R^2. Here, the "Pred R-Squared" of 0.9995 is in reasonable agreement with the Adj R-Squared of 0.9998. Adeq Precision measures the signal to noise ratio. A ratio greater than 4 is desirable. "Adeq precision" showed (R1, R2, R3, R4) was 260.621, 116.230, 91.903 and 379.858 indicates an adequate signalrespectively. This model can be used to navigate the design space.

These statistics are used to prevent over fitting of model.

Subsequentlyproducing the polynomial equations relating the dependent and independent variables, the process was optimized for the responses as shown in table 4. Mathematical optimization using the desirability approach was employed to locate the optimal settings of the process variables to obtain the desired responses. Optimized conditions were obtained by setting constraints on the dependent and independent variables. Optimization was performed to obtain the levels of A-C which maximize R2 and R3, minimize R1.

Table-5: ANOVA results of the quadratic model for the response % of CDR at 12 h (R2)

Source variations	Sum of Squares	DF	Mean Square	F Value	p-value Prob> F	R^2
Model	332.25	9	36.92	1439.65	< 0.0001	0.9995
A-Cholestrol	303.81	1	303.81	11847.79	< 0.0001	
B-Tween 80	7.61	1	7.61	296.57	< 0.0001	
C-Span 80	0.15	1	0.15	5.90	0.0455	
AB	0.16	1	0.16	6.24	0.0411	
AC	0.022	1	0.022	0.88	0.3801	
BC	3.61	1	3.61	140.78	< 0.0001	
A^2	16.72	1	16.72	651.88	< 0.0001	
B^2	0.019	1	0.019	0.75	0.4157	
C^2	2.368	1	2.368	9.236	0.9261	
Residual	0.18	7	0.026			
Lack of Fit	0.068	3	0.023	0.80	0.5536	

Table-6: ANOVA results of the quadratic model for the response % EE (R3)

Source variations	Sum of Squares	DF	Mean Square	F Value	p-value Prob> F	R^2
Model	433.28	3	144.43	1238.23	< 0.0001	0.9965
A-Cholesterol	432.18	1	432.18	3705.24	< 0.0001	
B-Tween 80	0.55	1	0.55	4.73	0.0488	
C-Span 80	0.55	1	0.55	4.73	0.0488	
Residual	1.52	13	0.12			
Lack of Fit	0.91	9	0.10	0.66	0.7205	

Table-7: ANOVA results of the quadratic model for the response viscosity (R4)

Source variations	Sum of Squares	DF	Mean Square	F Value	p-value Prob> F	R^2
Model	2.927	9	32522.98	18303.65	< 0.0001	0.9995
A-Cholesterol	2.922	1	2.922	1.645	< 0.0001	
B-Tween 80	14.04	1	14.04	7.90	0.0261	
C-Span 80	74.42	1	74.42	41.88	0.0003	
AB	16.81	1	16.81	9.46	0.0179	
AC	12.25	1	12.25	6.89	0.0341	
BC	210.25	1	210.25	118.33	< 0.0001	
A^2	0.056	1	0.056	0.031	0.8645	
B^2	73.74	1	73.74	41.50	0.0004	
C^2	66.86	1	66.86	37.63	0.0005	
Residual	12.44	7	1.78			
Lack of Fit	11.37	3	3.79	14.19	0.0134	

Table-4: Regression equation for the response

Response	Regression equation
R1	+892.60 +51.13 A – 1.63 B -0.75 C -1.25 AB -1.00AC + 0.50 BC -36.17 A^2 - 0.67 B^2 +0.075C^2
R2	+63.44 + 6.16 A +0.98 B -0.14 C +0.20AB -0.075AC +0.95 BC +1.99 A^2 +0.067 B^2 –7.500C^2
R3	+56.46 +7.35 A +0.26 B –0.26 C
R4	+306.22 +191.13 A +1.32 B +3.05 C +2.05 AB +1.75 AC -7.25 BC +0.12 A^2 - 4.18 B^2 –3.99 C^2

Table-8: Optimized values obtained by the constraints applies on R1 to R4

Independent variables	Values	Predicted values				Code	Observed values			
		P. size (R1)	% CDR (R2)	% EE (R3)	Viscosity cps (R4)		P. size	% CDR	% EE	Viscosity cps
Cholesterol	175	892.6	63.44	56.46	306.22	SM 5	893	63.3	56.7	305.4
Tween 80	300					SM11	892	63.5	56.3	306.3
Span 80	300					SM15	892	63.4	56.1	306.1

The mathematical model generated for % CDR (R2) was found to be significant with F-value of 1439.65 ($p < 0.0001$) and R^2 value of 0.9995. The independent variables A, B, C and the quadratic term of A^2 have significant effects on the % CDR, since the P-values less than 0.0500 represent the significant model terms as shown in Table 5. Results of the equation indicate that the effect of A, B, C, AB, BC, A^2 are more significant model. The influence of the main and interactive effects of independent variables on the % CDR was further elucidated using the perturbation and 3D response surface plots. The perturbation plot (Figure 23) showing the main effects of A, B and C on the percentage CDR (R2) of silymarin niosomes. This figure clearly shows that A&B has the main and the major effect on R2 followed by C which has a little effect on R2. The relationship between the dependent and independent variables was further elucidated using 2D response surface plots,3D response surface plot and 3-D cube plot are shown in (Figure 24, 25 and 26). Figure 25 shows the interactive effect of A and B on the % CDR (R2) at fixed level of C. At low levels of A (cholesterol), R2 increases from 58.6% to 59.4%. Similarly, at high levels of A, R2 increases from 70.5% to 72.8%.

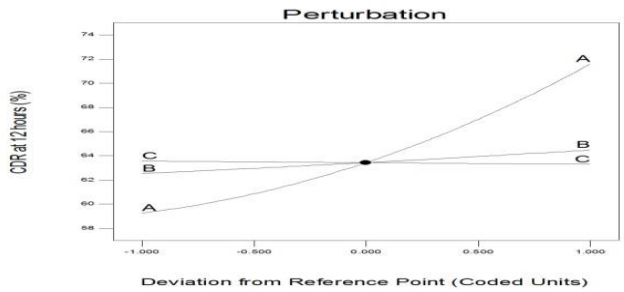

Figure-23: Perturbation plot showing the main effect of cholesterol (A),tween 80 (B) and span 80 (C) on % CDR(R2)

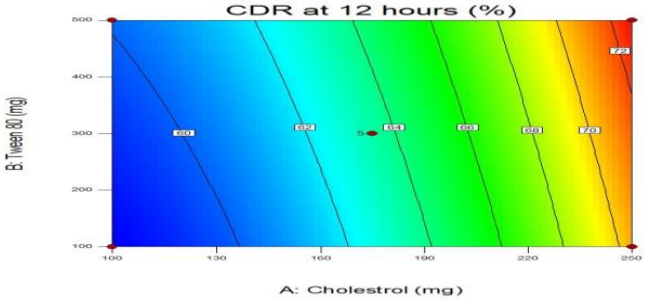

Figure-24: Response surface plot presenting the interactionbetween the cholesterol and tween 80 affecting the % CDR at constant span 80 concentration(R2).

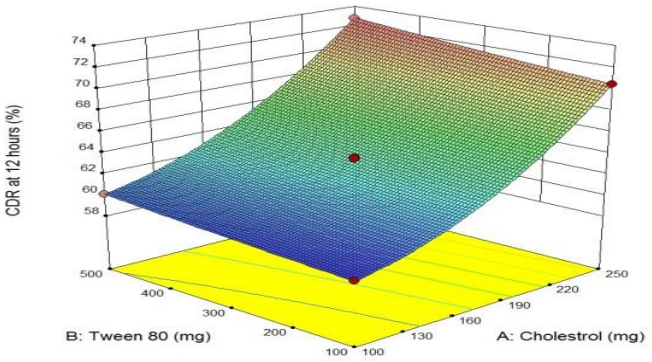

Figure-25: Response surface plot presenting the interaction between the cholesterol and tween 80 affecting the % CDR at constant span 80 concentration(R2).

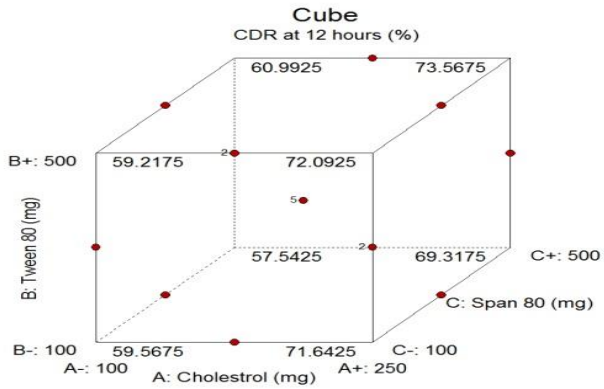

Figure -26: 3-D cube plot of Box-Behnken design (R2).

The accurate model produced for % EE (R3) was found to be significant with F-value of 1238.23 ($p < 0.0001$) and R^2 value of 0.9965. The independent variables A, B, C has significant effects on the % EE, since the P-values less than 0.0500 represent the significant model terms as shown in Table 6. The perturbation plot (Figure 27) showing the main effects of A, B and C on the percentage EE (R3) of silymarin niosomes. The correlationamong the dependent and independent variables was further elucidated using response surface plots, response surface plot and 3-D cube plot are shown in Figure. 28, 29 and 30. Figure 29 shows the interactive effect of A and B on the practical % EE (R3) at fixed level of C. At low levels of A (cholesterol), R3 increases from 49.2% to 56.7%. Similarly, at high levels of A, R3 increases from 63.3% to 64.2%.

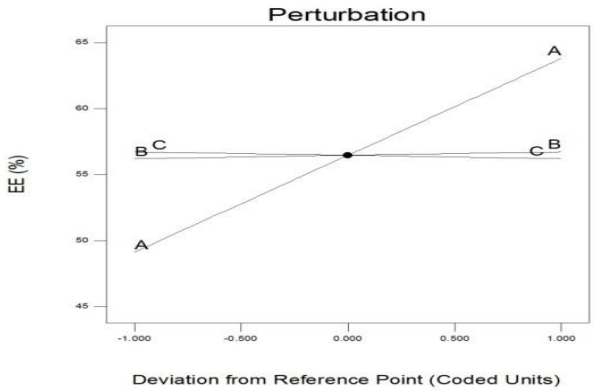

Figure-27: Perturbation plot showing the main effect of cholesterol (A), tween 80 (B) and span 80 (C) on % EE (R3)

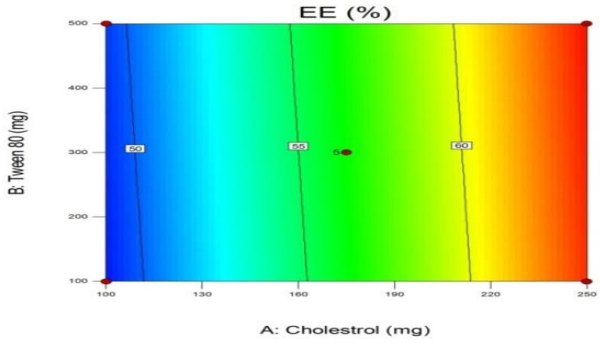

Figure-28: Response surface plot presenting the interaction between the cholesterol and tween 80affecting the % EE at constant span 80 concentration(R3).

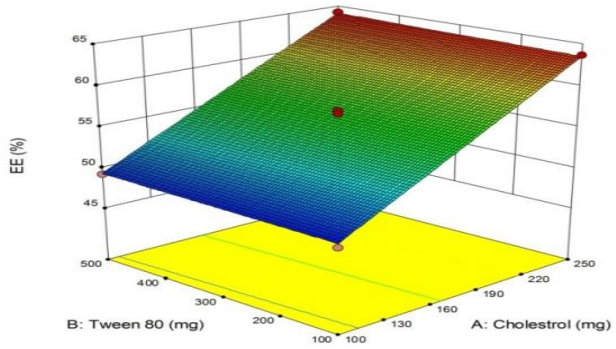

Figure-29: Response surface plot presenting theinteraction between the cholesterol and tween 80 affecting the % EE at constant span 80 concentration(R3).

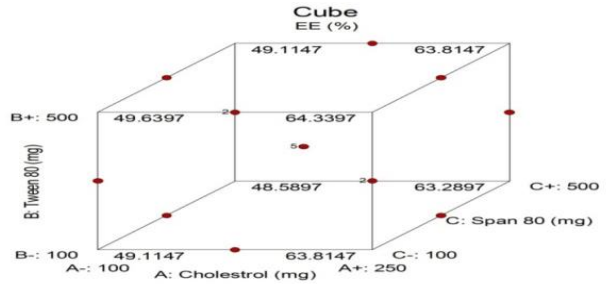

Figure -30: 3-D cube plot of Box-Behnken design (R3).

The accurate model produced for viscosity (R4) was found to be significant with F-value of 18303.65 ($p < 0.0001$) and R2 value of 0.9994. Since the P-values less than 0.0500 represent the significant model terms as shown in Table 7. In this case A, B, C, AB, AC, BC, B^2, and C^2 are significant model. The perturbation plot (Figure 31) showing the main effects of A, B and C on the viscosity (R4) of silymarin niosomes. The correlationamong the dependent and independent variables was further elucidated using response surface plots, response surface plot and 3-D cube plot are shown in Figure. 32, 33 and 34. Figure 33 shows the interactive effect of A and B on the viscosity (R4) at fixed level of C.

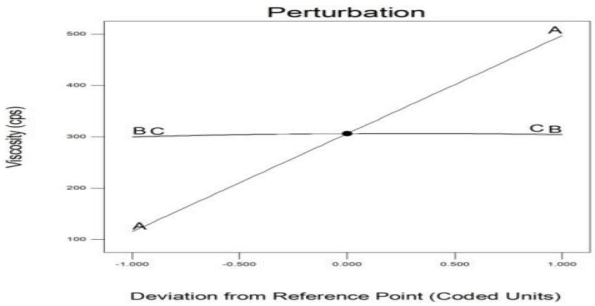

Figure-31: Perturbation plot showing the main effect of cholesterol (A), tween 80 (B) and span 80 (C) on viscosity (R4)

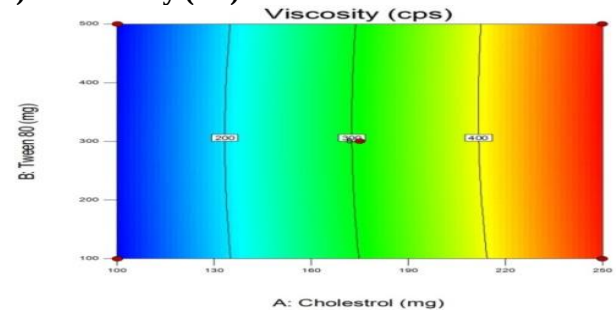

Figure-32: Response surface plot presenting the interaction between the cholesterol and tween 80 affecting the viscosityat constant span 80 concentration(R4).

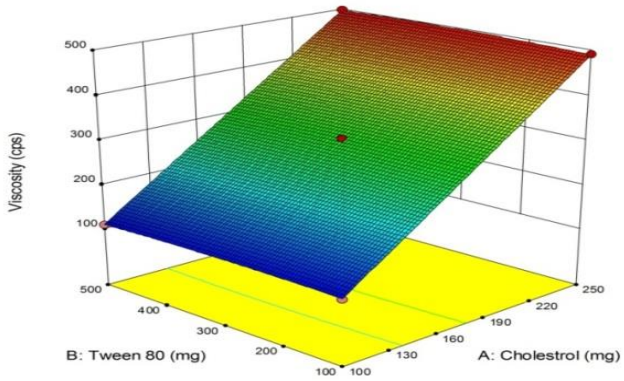

Figure-33: Response surface plot presenting the interactionbetween the cholesterol and tween 80 affecting the viscosityat constant span 80 concentration(R4).

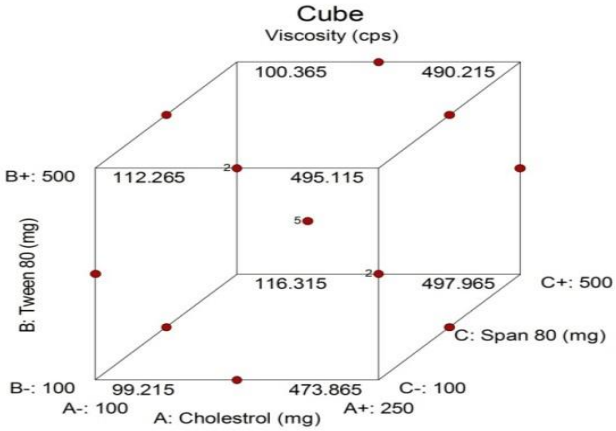

Figure -34: 3-D cube plot of Box-Behnken design (R4).

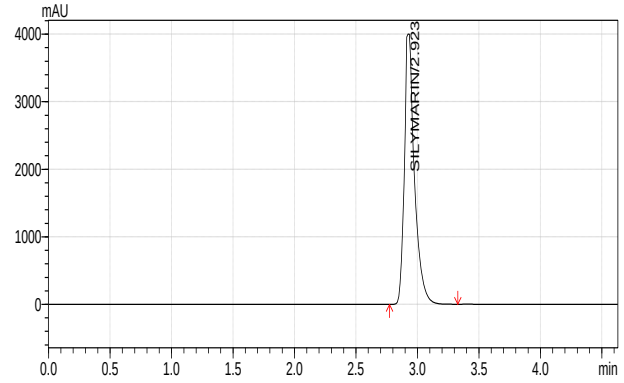

Figure -35: Typical chromatogram of silymarin

SM5, SM11 and SM15 batches code of silymarin niosomeswere prepared according to these optimized levels. Observed responses were in close agreement with the predicted values of the optimized process was shown in Table 8, thereby demonstrating the

feasibility. The cumulative drug release from niosomes at the end of 12th hour was shown in table 2.

CONCLUSION

The result of the silymarin loaded nanostructured lipid carriers has succeeded the objectives of particle size, % CDR, % entrapment efficiency and viscosity. The factorial equation for particle size exhibited a good correlation coefficient (1.000) and the Model F value of 10570.43 which implies the model is significant. Values of "Prob> F" less than 0.0500 indicate model terms are significant. In this case A, B, C and the quadratic term of A^2 are significant model. Externally studentized residual versus predicted pointe are scattered randomly between the outlier detection limits - 4.5 to + 4.5 and -3.5 to +3.5. The interactive effect of A and B on the % CDR (R3) at fixed level of C. At low levels of A (cholesterol), R3 increases from 49.2% to 56.7%. Similarly, at high levels of A, R3 increases from 63.3% to 64.2%.

REFERENCE:

[1] YP Pandey, G Sahni, A review on hepatoprotective activity of silymarin, Int. J.Res. Ayu. Pharm. 2: 75–79 (2011).

[2] S Srivastava, AK Srivastava, S Srivastava, GK Patnaik, BN Dhawan, Effect ofpicroliv and silymarin on liver regeneration in rats, Ind. J. Pharmacol. 26:19–22 (1994).

[3] SSrivastava, AK Srivastava, GK Patnaik, BN Dhawan, Effect of picrolivonliver regeneration in rats, Fitoterapia. 67: 252–256 (1996).

[4] L Mira, M Silva, CF Manso, Scavenging of reactive oxygen species by silibindihemisuccinate, Biochem. Pharmacol. 48:753–759 (1994).

[5] E Shaker, H Mahmoud, S Mnaa, Silymarin, the antioxidant component andsilybummarianum extract prevent liver damage, Food Chem. Tox. 48:803–806 (2010).

[6] HZ Toklu, T Tunali-Akbay, G Erkanli, M Yüksel, F Ercan, G Sener, Silymarin,the antioxidant component of Silybummarianum, protects againstburn-induced oxidative skin injury, Burns 33: 908–916 (2007).

[7] C Nencini, G Giorgi, L Micheli, Protective effect of silymarin on oxidativestress in rat brain, Phytomedicine 14:129–135 (2007).

[8] HZ Toklu, T TunaliAkbay, A Velioglu-Ogunc, F Ercan, N Gedik, MKeyer-Uysal, G Sener, Silymarin, the antioxidant component of Silybummarianum, prevents sepsis-induced acute lung and brain injury, J. Surg. Res.145: 214–222 (2008).

[9] A Svobodová, A Zdarilová, D Walterová, J Vostálová, FlavonolignansfromSilybummarianum moderate UVA-induced oxidative damage to HaCaTkeratinocytes, J. Dermatol. Sci. 48:213–224 (2007).

[10] S Dhanalakshmi, GU Mallikarjuna, RP Singh, R Agarwal, Dual efficacy of silibinin in protecting or enhancing ultraviolet B radiation-caused apoptosis in HaCaT human immortalized keratinocytes, Carcinogenesis 25: 99–106 (2004).

[11] TW Leonard, J Lynch, MJ McKenna, DJ Brayden. Promoting absorption of drugs in human's medium chain fatty acid-based solid dosage forms: GIPETTM. Exp. Opin.Drug.Deliv. 3: 685–692 (2006).

[12] IF Uchegbu, SP Vyas. Non-ionic surfactant based vesicles (niosomes) in drug delivery. Int. J. Pharm. 172, 33–70 (1998).

[13] JN Khandare, G Madhavi, BM Tamhankar. Niosomes novel drug delivery system.East. Pharm. 37: 61–64(1994).

[14] SM Bal, Z Ding, E van Riet, W Jiskoot, JA Bouwstra. Advances in transcutaneous vaccine delivery: do all ways lead to Rome? J. Control. Release 148: 266–282 (2010).

[15] C Dufes, F Gaillard, IF Uchegbu, AG Schätzlein, JCOlivier, JM Muller.Glucose-targeted niosomes deliver vasoactive intestinal peptide (VIP) to the brain. Int. J. Pharm. 285: 77–85(2004).

[16] CO Rentel, JA Bouwstra, B Naisbett, HE Junginger. Niosomes as a novel peroral vaccine delivery system. Int. J. Pharm. 186: 161–167 (1999).

[17] AS Guinedi, ND Mortada, S Mansour, RM Hathout. Preparation and evaluation of

reverse-phase evaporation and multilamellarniosomes as ophthalmic carriers of acetazolamide. Int. J. Pharm. 306: 71–82 (2005).

[18] C Marianecci, D Paolino, C Celia, M Fresta, M Carafa,F Alhaique. Nonionic surfactant vesicles in pulmonary glucocorticoid delivery: characterization and interaction with human lung fibroblasts. J. Control. Release 147: 127–135(2010).

[19] IA Alsarra, AA Bosela, SM Ahmed, GM Mahrous. Proniosomes as a drug carrier for transdermal delivery of ketorolac. Eur. J. Pharm. Biopharm. 59:485–490(2005).

[20] M Manconi, C Caddeo, C Sinico, D Valenti, MC Mostallino, G Biggio, AM Fadda. Ex vivo skin delivery of diclofenac by transcutol containing liposomes and suggested mechanism of vesicle–skin interaction. Eur. J. Pharm. Biopharm. 78: 27–35(2011).

[21] S Mura, M Manconi, C Sinico, D Valenti, AM Fadda. Penetration enhancer containing vesicles (PEVs) as carriers for cutaneous delivery of minoxidil. Int. J.Pharm. 380:72–79(2009).

[22] TeoJohnson , Jaya Raja Kumar , Hiew Mei Yi , Yeap Su Yong , A Kasturi. Factorial design of new surfactant “hibiscus rosasinensis leaf” for nanoparticles: glimepiride vs hibiscus rosasinensis. Rapports De Pharmacie 1(2):73-80 (2015).

[23] IF Uchegbu, R Duncan. Niosomes containing N-(2-hydroxypropyl)methacrylamide copolymer-doxorubicin (PK1): effect ofmethod of preparation and choice of surfactant on niosome characteristics anda preliminary study of body distribution. Int. J. Pharm. 155(1997).

[24] K Ruckmani, V Sankar. Formulation and optimization of Zidovudinenio-somes.AAPS PharmSciTech. 11:1119–1127(2010).

[25] L Tavano, M Vivacqua, V Carito, R Muzzalupo, MC Caroleo, F Nicoletta. Col-loidsSurf., B 102 (2013) 803.